

Chapter 19

Functional NIRS Measurement of Cytochrome-C-Oxidase Demonstrates a More Brain-Specific Marker of Frontal Lobe Activation Compared to the Haemoglobins

Isabel de Roever, Gemma Bale, Robert J. Cooper, and Ilias Tachtsidis

Abstract Functional near-infrared spectroscopy (fNIRS) is an increasingly common neuromonitoring technique used to observe evoked haemodynamic changes in the brain in response to a stimulus. The measurement is typically in terms of concentration changes of oxy- (ΔHbO_2) and deoxy- (ΔHHb) haemoglobin. However, noise from systemic fluctuations in the concentration of these chromophores can contaminate stimulus-evoked haemodynamic responses, leading to misinterpretation of results. Short-separation channels can be used to regress out extracerebral haemodynamics to better reveal cerebral changes, significantly improving the reliability of fNIRS. Broadband NIRS can be used to additionally monitor concentration changes of the oxidation state of cytochrome-c-oxidase (ΔoxCCO). Recent studies have shown ΔoxCCO to be a depth-dependent and hence brain-specific signal. This study aims to investigate whether ΔoxCCO can produce a more robust marker of functional activation. Continuous frontal lobe NIRS measurements were collected from 17 healthy adult volunteers. Short 1 cm source-detector separation channels were regressed from longer separation channels in order to minimise the extracerebral contribution to standard fNIRS channels. Significant changes in ΔHbO_2 and ΔHHb were seen at 1 cm channels but were not observed in ΔoxCCO . An improvement in the haemodynamic signals was achieved with regression of the 1 cm channel. Broadband NIRS-measured concentration changes of the oxidation state of cytochrome-c-oxidase has the potential to be an alternative and more brain-specific marker of functional activation.

Keywords Near-infrared spectroscopy • Functional activation • Cytochrome-c-oxidase • Haemodynamics • Short-separation regression

I. de Roever (✉) • G. Bale • R.J. Cooper • I. Tachtsidis
Department of Medical Physics and Bioengineering, University College London,
London, UK
e-mail: isabel.roever.13@ucl.ac.uk

1 Introduction

Functional near-infrared spectroscopy is commonly used to monitor stimulus-evoked cerebral haemodynamic responses due to neurovascular coupling, via measured regional concentration changes of oxygenated and deoxygenated haemoglobin. A typical functional activation haemodynamic response function consists of an increase in ΔHbO_2 and a concurrent, co-located decrease in ΔHHb . However, one of the main problems with fNIRS is its susceptibility to noise. This can arise from two main sources: task-related systemic activity and systemic-driven changes in the extracerebral layers [1]. The latter is a significant source of interference due to the nature of fNIRS measurements, where light propagates through the superficial layers upon emission and detection in reflectance mode, and hence is highly sensitive to changes in these superficial layers [2].

An increasingly common method to reduce contributions from extracerebral layers is with the use of short source-detector separation NIRS channels to sample only those layers, and use of the resulting signals as regressors in a linear model of the longer fNIRS channels [3]. It has been shown that a short source-detector separation of ~ 0.8 cm can effectively sample the extracerebral layer [2]. Hence, short channels can facilitate removal of superficial contamination from standard fNIRS channels, significantly improving the reliability of fNIRS measurements.

Using broadband NIRS we can additionally monitor oxidation changes of cytochrome-c-oxidase (CCO). CCO is the terminal electron acceptor in the electron transport chain in the mitochondria and is responsible for more than 95% of oxygen metabolism. Measurements of ΔoxCCO therefore provides information about oxygen utilisation at a cellular level [4]. The concentration of CCO is less than 10% *in vivo* than that of haemoglobin, hence a broadband NIRS system is required to accurately separate changes in attenuation due to this chromophore [5].

Recently, it has been shown using a broadband NIRS system with multiple source-detector separations that ΔoxCCO signals display a depth-dependence not seen in haemodynamic signals during oxygen delivery challenges in the healthy adult head [6]. The ΔoxCCO response was only seen at longer source-detector separations (3.5 cm) compared to ΔHbO_2 and ΔHHb , which showed a response at all source-detector separations (2, 2.5, 3 and 3.5 cm) interrogating both scalp and brain. This depth-dependence suggests CCO is brain-specific; this is likely due to the higher mitochondrial density in tissue with higher metabolic rates such as the brain compared to tissue with lower metabolic rates [6]. The ΔoxCCO signal therefore offers an alternative cerebral optical signal to haemodynamic signals.

This study aims to investigate the use of ΔoxCCO as an alternative and more robust marker of functional activation due to its brain-specificity compared to haemoglobin signals. The extracerebral contribution to the haemodynamic and metabolic signals is investigated with the use of a multi-distance broadband NIRS system, with short separation of 1 cm to probe mostly the skin, scalp and skull.

2 Methods

Healthy adult volunteers were recruited for this study and written informed consent obtained. The study was approved by the University College London (UCL) Ethics Committee. Data were collected from 17 healthy adult volunteers (13 male; age range 22–34 years) during functional activation. A working memory challenge in the form of either a Stroop task or anagram-solving task was used in order to induce a frontal haemodynamic response. Data were collected continuously for a 30 s baseline period, followed by 30 s of activation and 30 s of rest, alternated 4 times. The total acquisition time was therefore 270 s.

Data were collected using a broadband NIRS system called CYRIL (CYtochrome Research Instrument and appliCation), previously described [7]. It is an 8-channel system with two light emission fibres; optode holders were placed on the right and left sides of the forehead of each subject as shown in Fig. 19.1. Intensity data from the 4 cm channels displayed poor signal-to-noise ratio so were excluded from further analysis.

CYRIL is comprised of a white light source and a lens-based spectrometer with the capacity to collect light intensity data for 136 wavelengths between 771–906 nm at 1 Hz sampling rate. Measured changes in light attenuation were then converted to concentration changes of ΔHbO_2 , ΔHHb and ΔoxCCO using the UCLn algorithm [5]. As the differential pathlength factor is likely to vary across different source-detector separations, no pathlength was used. Instead, concentration data are presented in terms of $\mu\text{M}\cdot\text{cm}$.

Data analysis was carried out in MATLAB (Mathworks, USA) and using modified versions of functions from the HOMER2 NIRS processing package (<http://www.homer-fnirs.org>). Concentration data were zero-meaned and bandpass-filtered in the range [0.005 0.3] Hz, using a 5th order Butterworth filter, to remove physiological noise. The haemodynamic response was then extracted using one of two methods: the first was a block-average across all the events for all the subjects to

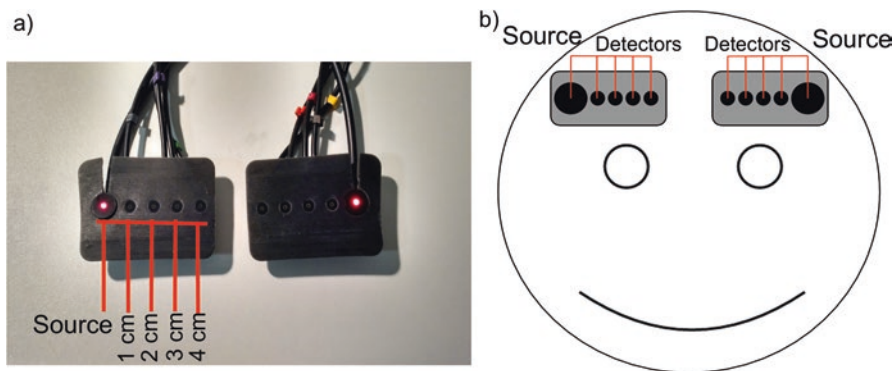


Fig. 19.1 (a) Probe holders with source and 4 detectors. (b) Diagram showing probe placement

isolate stimulus-related activations from uncorrelated haemodynamic trends ('block average method'); the second involved regression of the 1 cm channel by building a simple general linear model of each chromophore signal from the 2 and 3 cm channels ('short-separation regression method'). This general linear model uses a series of Gaussian basis functions convolved with a vector defining the time of the stimulus presentation to model the haemodynamic response function [8].

All statistical analysis was carried out in SPSS (IBM, USA). A baseline period was defined as the 10 s window immediately prior to the onset of activation, and 10 s activation period was chosen around the maximum change in the middle of the stimulus period. The response for each subject was defined as the difference between activation and baseline. Student's unpaired, one-sided t-test was used to compare the response of the activation compared to zero (i.e. no response) and values of $p < 0.05$ were considered significant. Results are presented as mean \pm standard error.

3 Results

The block average and short-separation regressed results for the 1, 2 and 3 cm channels are shown in Fig. 19.2.

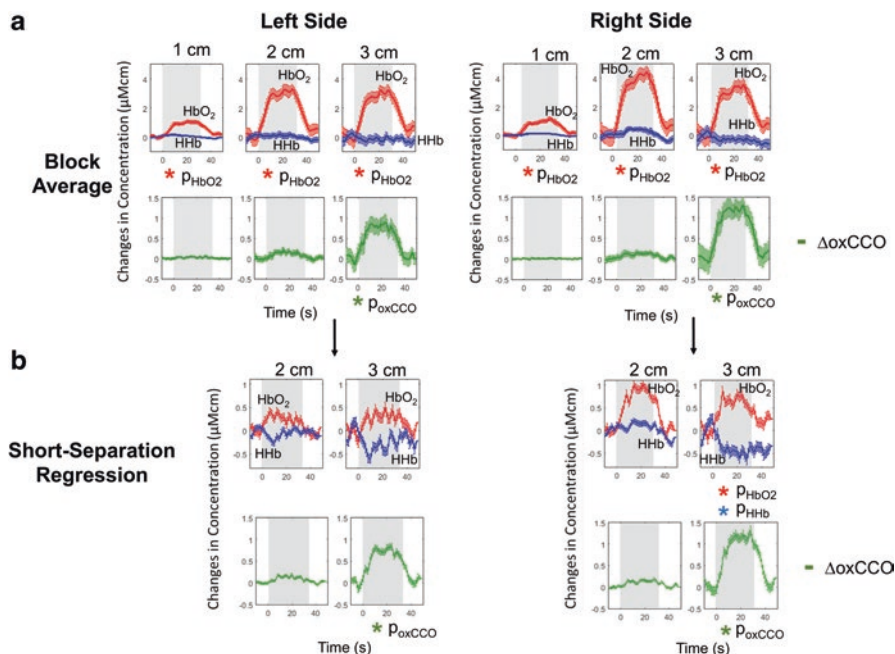


Fig. 19.2 Block-average and standard error of mean for 17 subjects during functional activation for left and right sides (a) without regression (b) with short-separation regression. Stimulus period indicated by grey background

Results of the block-average method for the right side show an increase in ΔHbO_2 at all source-detector separations, with a mean increase of $1.2 \pm 0.5 \mu\text{M}\cdot\text{cm}$ at 1 cm, $4.5 \pm 1.6 \mu\text{M}\cdot\text{cm}$ at 2 cm and $3.6 \pm 1.6 \mu\text{M}\cdot\text{cm}$ at 3 cm. No response is seen in ΔHHb at any of the channels. The ΔoxCCO shows no significant response at 1 cm and 2 cm but a large response is seen at 3 cm of $1.3 \pm 0.8 \mu\text{M}\cdot\text{cm}$. Results for the short-separation regression method show a significant increase in ΔHbO_2 at only 3 cm of $0.9 \pm 0.4 \mu\text{M}\cdot\text{cm}$, whilst ΔHHb now displays a significant decrease at 3 cm of $-0.6 \pm 0.5 \mu\text{M}\cdot\text{cm}$. The ΔoxCCO shows similar results as before, with the mean response of $1.3 \pm 0.4 \mu\text{M}\cdot\text{cm}$ at 3 cm.

Results for the block-average method for the left side show an increase in ΔHbO_2 at all separations, with mean values of $1.1 \pm 0.4 \mu\text{M}\cdot\text{cm}$ at 1 cm, $3.3 \pm 1.3 \mu\text{M}\cdot\text{cm}$ at 2 cm and $3.2 \pm 1.5 \mu\text{M}\cdot\text{cm}$ at 3 cm. There is no significant change in ΔHHb at any of the separations. ΔoxCCO shows a significant increase at only the 3 cm channel of $0.9 \pm 0.8 \mu\text{M}\cdot\text{cm}$. After short-separation regression, no significant changes are seen in either of the haemodynamic variables. ΔoxCCO displays a similar response as to the block average, with a significant increase of $0.8 \pm 0.3 \mu\text{M}\cdot\text{cm}$ at 3 cm.

4 Discussion

We observed a response in ΔoxCCO in only the longer source-detector separation of 3 cm but not in the shorter separations of 1 cm and 2 cm. The regression of the 1 cm channel made no difference to the ΔoxCCO response.

There was a response in ΔHbO_2 at all source-detector separations, whereas ΔHHb showed no significant changes in any of the channels. After short-separation regression, the 2 cm channel did not show any significant response in the ΔHbO_2 and ΔHHb signals for either side, whilst at 3 cm there was a significant increase in ΔHbO_2 and decrease in ΔHHb for the right side and a similar but not significant trend was seen for the left side.

A scalp response was seen in both the right and left sides in the 1 cm channel. Results for the right side block-average at 3 cm show a false negative; no functional activation observed from the haemodynamic signals due to the absence of a significant decrease in ΔHHb . However, ΔoxCCO shows a strong increase that is indicative of functional activation. When the 1 cm short separation is regressed from the longer channels, we see a functional response in the haemoglobins not previously seen, with a significant increase in ΔHbO_2 and now significant decrease in ΔHHb . If only the changes in ΔHbO_2 were reported, then at 1 cm and 2 cm one would observe functional activation; however, taking into account ΔoxCCO and the short-separation regressed ΔHHb signals, we observe no functional activation in these channels. In this case, the ΔoxCCO and regressed ΔHHb signals have the capacity to rule out false positives.

Results for the left hemisphere show no functional activation from the haemoglobin signals at 3 cm even after regression. If we rely on the significant increase in ΔoxCCO as an indicator of functional activation, the haemodynamic result is a false

negative. The 1 cm short-separation regression in this case did not have the capacity to recover the false negative in the haemodynamic signals, which may be due to the scalp response not being fully removed. A false negative could also be caused by systemic changes such as blood pressure producing a significant effect on the brain physiology that masked activation. We did not measure systemic variables so cannot comment on the cause. However, previous studies have found systemic task-related changes to influence NIRS signals [9].

Note that the amplitude of the haemoglobin signals is on a similar scale to that of the ΔoxCCO signals after regression. This could be due to the fundamental characteristics of the regression method. The least-squares static estimator regression approach employed here can result in an underestimation of the haemodynamic response: either because the short-separation measurement has a non-negligible sensitivity to cortical tissue or because the superficial short-separation signal during the functional response mimics the true cerebral response. This effect could likely be improved through the use of a dynamic estimation approach, such as the Kalman filter methodology employed by Gagnon et al. [10].

This study demonstrates that inclusion of the ΔoxCCO signal during functional activation studies with fNIRS can provide an additional robust marker of brain activation allowing better identification of false positives and negatives.

Acknowledgments The authors would like to thank the Centre for Doctoral Training Integrated Photonic and Electronic Systems (EP/L015455/1) and The Wellcome Trust (104580/Z/14/Z) for the financial support of this work. RJC is funded by EPSRC fellowship EP/N025946/1.

References

1. Tachtsidis I, Scholkmann F (2016) False positives and false negatives in functional near-infrared spectroscopy : issues, challenges, and the way forward. *Neurophotonics* 3:030401–1–030401–6
2. Brigadoi S, Cooper RJ (2015) How short is short? Optimum source–detector distance for short-separation channels in functional near-infrared spectroscopy. *Neurophotonics* 2:025005–1–02005–9
3. Saager RB, Telleri NL, Berger AJ (2011) Two-detector corrected near infrared spectroscopy (C-NIRS) detects hemodynamic activation responses more robustly than single-detector NIRS. *NeuroImage* 55:1679–1685
4. Bainbridge A, Tachtsidis I, Faulkner SD et al (2013) Brain mitochondrial oxidative metabolism during and after cerebral hypoxia-ischemia studied by simultaneous phosphorus magnetic-resonance and broadband near-infrared spectroscopy. *NeuroImage* 102:173–183
5. Bale G, Elwell CE, Tachtsidis I (2016) From Jöbsis to the present day: a review of clinical near-infrared spectroscopy measurements of cerebral cytochrome-c-oxidase. *J Biomed Opt* 21:091307–1–091307–18
6. Kolyva C, Ghosh A, Tachtsidis I et al (2014) Cytochrome c oxidase response to changes in cerebral oxygen delivery in the adult brain shows higher brain-specificity than haemoglobin. *NeuroImage* 85:234–244

7. Bale G, Mitra S, Meek J et al (2014) A new broadband near-infrared spectroscopy system for in-vivo measurements of cerebral cytochrome-c-oxidase changes in neonatal brain injury. *Biomed Opt Express* 5:663–676
8. Gagnon L, Cooper RJ, Yücel M et al (2012) Short separation channel location impacts the performance of short channel regression in NIRS. *NeuroImage* 59:2518–2528
9. Tachtsidis I, Leung TS, Devoto L et al (2008) Measurement of frontal lobe functional activation and related systemic effects: a near infrared spectroscopy investigation. *Adv Exp Med Biol* 614:397–403
10. Gagnon L, Perdue K, Greve DN et al (2011) Improved recovery of the hemodynamic response in diffuse optical imaging using short optode separations and state-space modeling. *NeuroImage* 56:1362–1371

Open Access This chapter is licensed under the terms of the Creative Commons Attribution 4.0 International License (<http://creativecommons.org/licenses/by/4.0/>), which permits use, sharing, adaptation, distribution and reproduction in any medium or format, as long as you give appropriate credit to the original author(s) and the source, provide a link to the Creative Commons license and indicate if changes were made.

The images or other third party material in this chapter are included in the chapter's Creative Commons license, unless indicated otherwise in a credit line to the material. If material is not included in the chapter's Creative Commons license and your intended use is not permitted by statutory regulation or exceeds the permitted use, you will need to obtain permission directly from the copyright holder.

